Chalcogenide Letters Vol. 13, No. 10, October 2016, p. 443 - 450

TAILORING THE STRUCTURAL AND OPTICAL PROPERTIES OF CdZnS THIN FILMS BY VACUUM ANNEALING

A. BAKHSH[a*], I. H. GUL[a], A. MAQSOOD[b], C. H. CHAN[c], S. H. WU[c], Y. C. CHANG[c]

[a]*Materials Engineering Department, School of Chemical and Materials Engineering (SCME), National University of Sciences and Technology (NUST), Islamabad, 44000, Pakistan*

[b]*Nano-Scale Physics Lab, Air University, Islamabad, 44000, Pakistan*

[c]*Research Center for Applied Sciences (RCAS), Academia Sinica, Taipei,11529, Taiwan*

Effect of vacuum annealing on structural and optical properties of CdZnS thin films is reported. Nano-crystalline CdZnS films have been deposited through sublimation technique and subsequently vacuum annealed at 300 ^{0}C and 400 ^{0}C for two hours. The samples have been characterized through X-ray diffraction, Scanning Electron Microscopy, Raman Scattering, UV-Visible spectroscopy and Photoluminescence. New diffraction peaks along (002) and (103) planes have been observed after vacuum annealing the polycrystalline thin films. Sample annealed at 400 ^{0}C revealed that large grains were made up of uniformly distributed tinier grains. Raman spectroscopy confirmed the existence of ZnS along with CdZnS and a decrease in substitution disorder due to Zn diffusion in the crystal structure with vacuum annealing. The band gap energy increased from 2.56 eV to 2.70 eV with a decrease in CdS enriched phase. Photoluminescence peaks exhibited a blue shift and Stoke's shift energy increased from 160 meV to 230 meV as a result of the vacuum annealing process.

(Received July 28, 2016; Accepted October 1, 2016)

Keywords: Cadmium Zinc Sulfide; Vacuum Annealing; Phonon; Photoluminescence; Optical Properties

1. Introduction

II–VI semiconductors have achieved attention of research community due to their tunable energy band gaps. The ternary and quaternary alloys of these compounds can be formed with a direct fundamental band gap entirely dependent upon alloy composition range. Wide-band gap and high absorption coefficients make these materials potential candidates for solar cell and optoelectronic applications[1]. Among II-VI semiconductors, CdZnS is a prominent ternary alloy with tunable optical and electrical properties controlled by constituent mole fraction, particle sizes and morphologies. The large exciton binding energies of CdS (29 meV) and ZnS (40 meV) enable the observation of excitonic emission at room temperature [2]. This encourages investigating the potential use of CdZnS in the exciton based optoelectronics devices. During the sublimation process, Zn diffusion in CdS forms ternary CdZnS compound with a direct energy band gap over the whole alloy composition [3] and is primarily dependent on a relative Cd:Zn ratio [4]. Thin films of CdZnS with a higher-energy band gap than CdS are candidates for window layers in solar cells [3]. The deposition of CdZnS at an elevated temperature may result into stoichiometric deviancies [5] and presence of some constituent materials like ZnS or CdS. This strongly affects the structural and optical properties of CdZnS thin films. The use of CdZnS in new optoelectronic devices demands controllable distribution of Zn content throughout the thin film. In order to

*Corresponding author: allah_bakhsh@scme.nust.edu.pk

achieve the desired structural and optical properties the fabricated thin films must undergo post deposition heat treatment [6] letting a uniform distribution of Zn content in crystal structure.

In this paper, we investigated the effects of vacuum annealing on the structural and optical properties of CdZnS thin films fabricated through mixing and sublimation technique. The samples have been characterized through X-ray diffraction, Scanning Electron Microscopy, Raman Scattering, UV-visible absorption spectroscopy and Photoluminescence measurements. The results show that high-temperature vacuum annealing can simultaneously modify the structural and optical properties in CdZnS thin films.

2. Experimental details

Thin films have been fabricated using the Closed Space Sublimation (CSS) technique. Mechanical mixed powder of 99.99% pure CdS and ZnS powders are used as source material. A graphite boat containing source material has been placed inside a vacuum chamber containing a substrate. The source and substrate were separate by a distance of 3.5 mm and mica sheet has been used to create a temperature gradient between them. Prior to heating, the system has been flushed with nitrogen gas to eliminate O_2 and any residual contaminations. Finally, the chamber was evacuated to a base pressure of 2×10^{-2} mbar using a mechanical rotary pump. CdZnS thin films were deposited on ITO coated glass substrate, before the fabrication process substrates were first washed with detergent and then sonicated in acetone and isopropanol alcohol (IPA) respectively for 30 minutes. The substrates have been dried with nitrogen air before loading them in the CSS chamber. Source and substrate have been heated directly by two halogen lamps. The temperatures are controlled with two temperature controllers connected through K-type thermocouples. The source and substrate have been heated up to 600 ^{0}C and 450 ^{0}C, for a deposition time of 3 minutes. After the deposition time attained, one sample has been left for cooling to room temperature and designated as SA, while for samples SB and SC, substrate temperatures have been reduced to 300 ^{0}C and 400 ^{0}C respectively, and samples left for vacuum annealing at this temperature for two hours.

The CdZnS thin films have been characterized by X-ray diffraction (Cu K-alpha radiation λ=1.54056Å), scanning electron microscopy (JEOL-instrument JSM-6490A) and UV–vis–NIR spectrophotometer (UV-2800). Raman and Photoluminescence measurements have been performed using He-Ne (633 nm) and He-Cd (325 nm) lasers sources respectively. Thickness of samples has been measured using NANOVEA PS50 optical profilometer and thickness is found to be 280 nm, 270 nm and 255 nm for sample SA, SB and SC. Thin films were uniform and showed good adhesion to the substrate.

3. Results and discussion

The crystalline structure and quality of CdZnS thin films are measured using X-ray diffraction technique in the 2θ angle ranging from 20^0 to 80^0. The XRD spectrum of samples (Figure 1) shows the peaks at 2θ equal to 26.41^0, 28.04^0, 47.74^0, 50.63^0 and 60.14^0 having preferred orientation along the (002), (101), (103), (200) and (104) planes for CdZnS, while (211), (222), and (400) are the characteristic's peaks of ITO. XRD patterns agreed with ICDD data card no. 00-049-1302 and 00-039-1058.

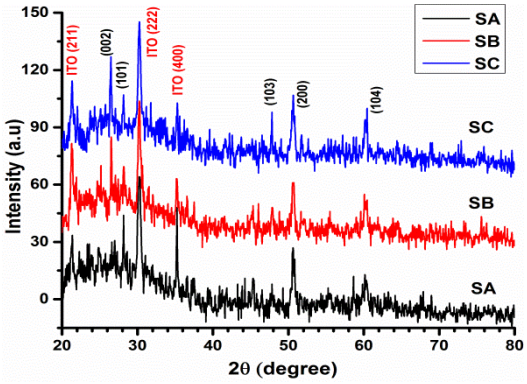

Fig. 1: XRD pattern of as deposited CdZnS thin film (SA) and samples annealed at 300 ^{0}C (SB) and 400 ^{0}C (SC) for two hours

XRD patterns confirmed that CdZnS thin films are polycrystalline with hexagonal crystal structure. No significant peak shift has been observed during annealing process; while the intensity increased along (002) and (104) planes and a new peak appeared along (103) for sample SC. XRD results confirmed the CdZnS composition for all the samples and increase in crystallinity with the annealing process. The average crystalline size (D) of the sample is estimated using Scherrer's formula [7]:

$$D = 0.94\lambda/\beta Cos\theta \quad (1)$$

Where, λ is the wavelength of X-ray used (λ = 1.54090Å), β is the full width at half maxima measured in radians and θ is the diffraction angle. The dislocation density (δ), the number of crystallites per unit area (N) and the strain (ε) of the films are determined by relations [8].

$$\delta = 1/D^2 \quad (2)$$

$$\varepsilon = \beta Cos\theta/4 \quad (3)$$

The estimated structural parameters are presented in table 1. The annealing process resulted into decrease in lattice parameters c from 6.783 Å to 6.724 Å while crystallite size increased from 35.1 nm to 75.4 nm with annealing process. Because of the high-temperature gradient between the source and substrate, material accumulated instantly on substrate surface resulting into stoichiometric in-homogeneity as well as deposition of some non-reacted constituent material (ZnS/CdS) underneath the CdZnS thin film. The annealing process resulted into decrease in dislocation density and lattice strain.

Table 1. Structural parameters of as deposited and annealed CdZnS thin films.

Sample Description	Annealing Temperature	a=b (nm)	c (nm)	Crystallite Size (D) (nm)	Dislocation Density δ (lines/m^2)	Strain (%)
SA	As deposited	0.4163	0.6783	35.1	8.11x10^{14}	0.409
SB	300 ^{0}C	0.4159	0.6718	41.7	5.75x10^{14}	0.386
SC	400 ^{0}C	0.416	0.6724	76.3	1.71x10^{14}	0.351

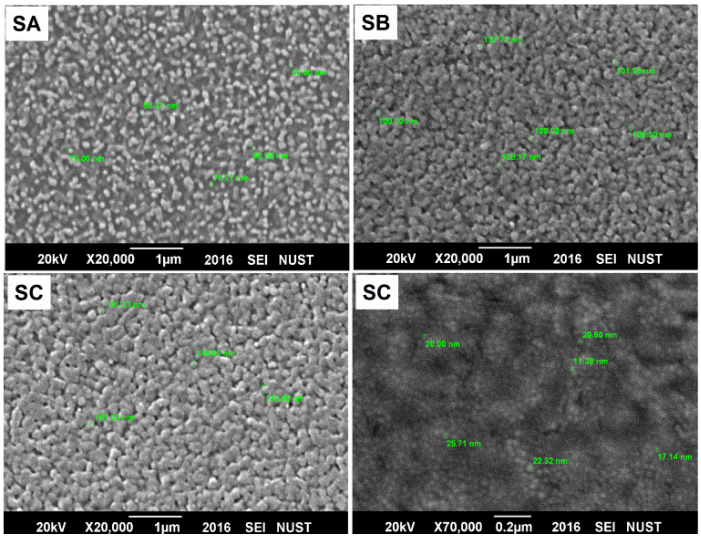

Fig. 2: SEM micrographs of as deposited CdZnS thin film (SA) and sample vacuum annealed at 300 ^{0}C (SB) and 400 ^{0}C (SC) for two hours.

Scanning electron microscopy (SEM) is an appropriate technique to analyze the surface morphology of thin films. SEM micrographs of as the deposited and samples annealed at 300 ^{0}C, and 400 ^{0}C for two hours are shown in Fig. 2. SEM micrographs revealed that thin films were homogenous and free from the cracks. The SEM micrograph of as the deposited sample SA showed the existence of isolated grains with a mean size of 70 nm. An increase in the grain size has been observed with the annealing process due to the inclusion of small grains into larger grains. An average grain size of 100 nm and 150 nm has been observed for samples SB and SC respectively. For Sample SC annealed at 400 ^{0}C for two-hour, it has been observed that large grains are composed of tinier grain with mean size of 20 nm. For samples SA and SB these smaller grains are not observable. It can be assumed that either these small initial grains are present in as the deposit sample which increased with annealing. Alternatively, they have been created due to evaporation of sulfur or ZnS after under vacuum annealing at 400 ^{0}C for two hours. These smaller grains can act as trap sites for excitons and charge carriers and influence the optical properties of CdZnS thin film.

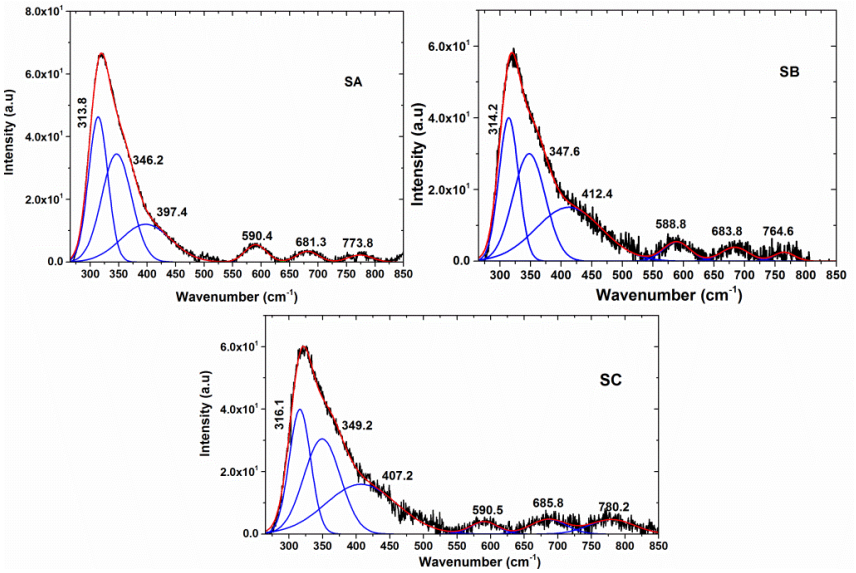

Fig. 3: Raman Spectra of as deposited (SA) CdZnS thin film and samples annealed at 300 ^{0}C (SB) and 400 ^{0}C (SC) for two hours.

Raman spectroscopy is one of the essential tools in the structural characterization of the materials. The crystalline quality and presence of ZnS have been identified through Raman's measurements. Fig. 3 shows the Raman spectra of CdZnS thin films collected with 633 nm excitation laser source. The peaks are further resolved through Origin software using Gaussian function. A Raman spectrum has been evaluated upon the basis of phonon peak position, Full Width at Half Maximum (FWHM) of the peak and peak line shape. The peak positions with FWHM for samples SA, SB and SC are summarized in table 2. For bulk CdS and ZnS Longitudinal Optical (1LO) phonon mode peaks exist at 300 cm^{-1} and 350 cm^{-1} respectively [9, 10]. The peak position of LO mode varies with the composition of Zn atoms within the CdS crystal structure. For the sample SA, SB and SC, first peak has been observed at 313.8 cm^{-1}, 314.2 cm^{-1} and 316.2 cm^{-1} with FWHM of 39.72 cm^{-1}, 37.63 cm^{-1} and 37.56 cm^{-1} respectively. These peaks are at higher wavenumbers than the bulk CdS (300 cm^{-1}) 1LO peak and recognized as CdZnS longitudinal optical (LO) phonon peaks. FWHM values (large/small) and behavior (increasing/decreasing) gives valuable information about the Raman spectra. In mixed crystals, it has been observed that substitution disorder results into broad spectra [11]. Large values of FWHM are the representations of substitution disorder in CdZnS crystal structure due to the existence of ZnS. The decrease in FWHM shows that the annealing process resulted into the decrease in substitution disorder. The second Raman peak in all the samples has been observed at 346.2 cm^{-1}, 347.6 cm^{-1} and 349.2 cm^{-1} with FWHM of 61.62 cm^{-1}, 62.11 cm^{-1} and 64.03 cm^{-1} respectively. This peak is recognized as the ZnS first LO mode peaks and confirmed the presence of ZnS material along with the CdZnS.

Nandakumar has reported an increase in FWHM with the decrease in particle size of CdS nanocrystals[12], while Sahoo at el have attributed the broadening arising from the phonon confinement in CdZnS nanocrystals[11]. The FWHM for ZnS peak increased with the annealing, indicating the decrease in ZnS particle size. Both the peaks shifted towards higher wavenumbers at 316.1 cm^{-1} and 349.2 cm^{-1} with annealing. This peak shift can be assigned to the adjusting of Zn in crystal structure, which shifted peak towards the higher wavenumber side. The origin of the peak near 397.4 cm^{-1} is not yet clear, and it is not reported in literature as for as our knowledge goes. The peaks at 590.4 cm^{-1} and 681.3 cm^{-1} of sample SA can assign to the modified second harmonic of 2-LO phonon of CdS (600 cm^{-1}) and ZnS (700 cm^{-1}) respectively. The existence of 1LO and 2LO phonon mode confirms the presence of highly crystalline material. The less intense peak at 773.8 cm^{-1} can be assigned to the multi-phonon peak. The Zn diffusion in crystal structure also resulted into a more asymmetric line shape towards a higher-energy side. FWHM increases inversely with the particle size and line shape becomes unsymmetrical if there are confinement effects[11]. Considering the increased FWHM of ZnS peaks along with the asymmetric line shape of Raman spectra it can be concluded that with the annealing process, ZnS particle size is decreasing and contributing to the quantum confinement effects in CdZnS system.

Table 2: Raman peak positions and FWHM of Raman peaks of as deposited and CdZnS thin films annealed at 300 ^{0}C and 400 ^{0}C for two hours.

Sample Description	Annealing Temperature	Peak Position Wavenumber (cm^{-1})	FWHM Wavenumber (cm^{-1})
SA	As deposited	313.8	39.72
		346.2	61.62
		397.4	103.18
		590.4	44.57
		681.3	45.45
		773.8	49.92
SB	Annealed at 300 ^{0}C	314.2	37.63
		347.6	62.11
		412.4	126.93
		588.8	52.19
		683.8	53.74
		764.6	40.20
SC	Annealed at 400 ^{0}C	316.1	37.56
		349.2	64.03
		407.2	125.25
		590.5	47.62
		685.8	62.41
		780.2	79.26

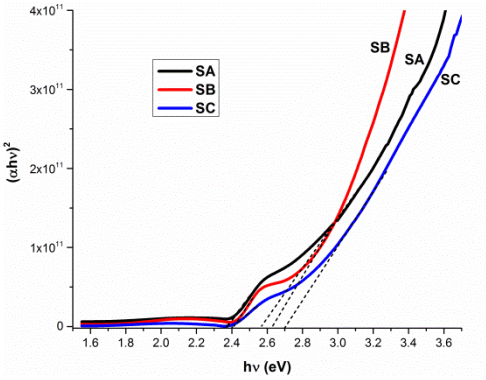

Fig. 4: Relation between $(\alpha h\nu)^2$ and $h\nu$ for as deposited and annealed CdZnS thin film samples.

The bandgap of materials offers useful information to examine features concerning with their band structures. In the present study, band gap (E_g) of samples is measured through absorption spectroscopy. Measurements are made in the 350 nm to 1000 nm wavelength range using ITO as reference. To measure the energy band gap from absorption spectra Tauc relation is used [8].

$$\alpha h\nu \propto (h\nu - E_g)^m \tag{5}$$

Where α is the absorption coefficient, hν is photon energy, E_g is the band gap of the thin films, and the exponent n = 1/2 for direct band gap material. The nature of the band gap is determined by plotting $(\alpha h\nu)^2$ vs hν and is shown in Fig. 4. The linearity of the curve confirmed the direct band transition of CdZnS thin film. The energy band gap of samples is estimated by extrapolating the linear portion of the curve to the photon energy axis for zero absorption coefficients. The intercept of the curve gives the optical band gap of thin film. For as grown and annealed samples, two distinct linear regions appear with two different band gap values designated as Eg_1 (low) and Eg_2 (high). Eg_1 bandgap energies are recorded at 2.37 eV, 2.39 eV and 2.40 eV for sample SA, SB and

SC respectively. These energies are close to the band gap energy of CdS (2.41 eV), which may arise due to formation of some Cd enriched phase in the samples. A decrease in this Cd enriched phase has been observed with the annealing process. The Eg_2 bandgap energies are recorded at 2.56 eV, 2.62 eV and 2.70 eV for samples SA, SB and SC respectively. Compared with the bandgap of CdS an increase in bandgap confirmed the formation of CdZnS compound. The annealing dependent increase in CdZnS bandgap can be assigned to the diffusion of Zn and the possible quantum confinement effect due to smaller particle size of ZnS shown by Raman measurements.

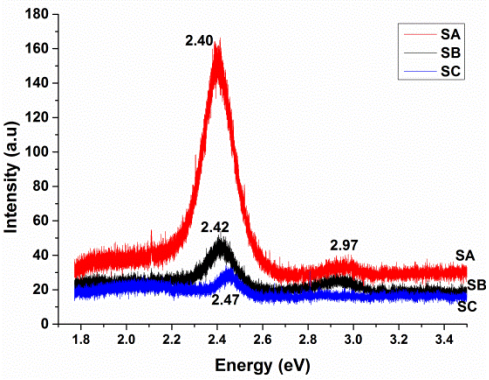

Fig. 5: Photoluminescence spectra of as deposited (SA) CdZnS thin film and thin film annealed at 300^{0}C (SB) and 400^{0}C (SC) for two hours

Fig. 5 shows the Photoluminescence (PL) spectra of samples SA, SB and SC. As the grown sample SA displayed strong emission in the green light region. Photoluminescence peak has been observed at 2.40 eV, 2.42 eV and 2.47 eV wavelengths for sample SA, SB and SC respectively. Compared with sample SA, a blue shift of 22 meV and 70 meV has been observed in the sample SB and SC. These peaks resulted from the non-radiative recombination process of photon-excited non-equilibrium carriers [9] and are related to near band edge emission of CdZnS [13]. In the samples SA and SB, a high-energy peak with low intensity has been observed at 2.97 eV. This peak can be assigned to the ZnS-related emission peaks associated with 346 cm^{-1} and 347 cm^{-1} Raman peaks of both the samples. This peak was absent in the sample SC annealed at 400 ^{0}C representing the reduction of ZnS in the sample. Stoke's shift is the difference between band gap energy and photoluminescence peak energy of CdZnS thin films. The Stoke's shift has been found to increase from 160 meV for sample SA to 200 meV and 230 meV for sample SB and SC. The Stoke's shift increase can be attributed to the improved Zn diffusion creating trap sites for excitons and charge carriers. The large Stoke's shift can reduce the reabsorption losses for light emission applications through prolong propagation of the emitted light within the material[14, 15]. The decrease in Photoluminescence intensity results due to more excitons bounded to trap sites. For as the deposited sample, more electron hole-pairs are available for emission giving rise to the emission intensity. No obvious Deep-Level Emission (DLE) peak has been observed in the low-energy region. The exciton emission peak is observable only if the long-range Coulomb coupling exists between the electron and hole. The observation of the exciton emission and associated LO phonon, confirms the highly crystalline nature of the CdZnS thin films [16].

4. Conclusions

In Summary, we have successfully fabricated CdZnS thin films on ITO coated glass slides through closed space sublimation technique. All the samples exhibited a hexagonal crystal structure, and XRD peak intensity increased along (002) and (104) planes for the annealed samples. A new diffraction peak emerged along (103) plane for sample SC annealed at 400 ^{0}C for two hours. Increase in crystallite size and decrease in strain and dislocation density was observed

with annealing process. Morphology shows that the grains are distributed uniformly, and grain size increased with the annealing. Raman spectroscopy confirmed the presence of CdZnS and ZnS-related optical phonon modes, with large FWHM values representing the substitution disorder and small particle size of ZnS. A decrease has been observed in substitution disorder and ZnS particle size with vacuum annealing process. The bandgap energies increased from 2.56 eV to 2.70 eV with vacuum annealing of CdZnS thin film at 400 ^{0}C for two hours. Photoluminescence peaks exhibited a blue energy shift with the vacuum annealing process. The samples SA and SB showed both CdZnS and ZnS emission peaks while the sample SC annealed at 400 ^{0}C showed only the CdZnS emission peak. Stoke's shift increased, and emission intensity decreased with the vacuum annealing process. Results showed that the structural and optical properties of CdZnS thin films are strongly influenced by vacuum annealing.

Acknowledgements

This work was supported by the Higher-Education Commission of Pakistan through IRSIP program [Case No:I-8/HEC/HRD/2015/4013]; and Pakistan Science Foundation [PSF/NUST-(136)].

References

[1] S.Saravanakumar, T. P. Kumar, K. Sankaranarayanan. Applied Surface Science, 257 (2011).
[2] J.Z. Muhammad Iqbal Bakti Utama, Rui Chen, Xinlong Xu, Dehui Li, Handong Sun and Qihua Xiong. Nanoscale 4 (2012).
[3] N.A.Shah. Waqar Mahmood. Optical Materials 36 (2014).
[4] T.Caijuan, Di Xia, T. Rongzhe, Li Wei, F. Lianghuan, Z. Jingquan, Wu Lili, Lei Zhi. Journal of Semiconductors 32 (2011).
[5] A.Romanyuk, O. Kolomys, V. Strelchuk, G. Lashkarev, O. Khyzhun, I. Timofeeva, V. Lazorenko, V. Khomyak. Semiconductor Physics, Quantum Electronics & Optoelectronics 17 (2014).
[6] F.E.Ghodsi, A. Abdolahzadeh Ziabari. Materials Science in Semiconductor Processing 16 (2013).
[7] Z. Akram K.S.Aqili, AsghariMaqsood. Journal ofCrystalGrowth 317 (2011).
[8] A.H.Reshak. Y. Al-Douri. Optik 126 (2015).
[9] L.V.Titova, T. B. Hoang, A. Mishra, L. M. Smith, H. E. Jackson, K.Y. Lee, H. Rho, J. M. Yarrison-Rice, Y.J. Choi, K. J. Choi, J.G. Park. Appl. Phys. Lett. 92 (2008).
[10] R.S.Castillo-Ojeda, J. Díaz-Reyes, R. Sanchez-Espíndola, M. Galvan-Arellano, O. Zaca-Moran. Current Applied Physics 15 (2015).
[11] S.Dhara. Satyaprakash Sahoo, V. Sivasubramanian, S. Kalavathi and A. K. Arora. J. Raman Spectrosc. 40 (2009).
[12] C.Vijayan, P. Nandakumar, M. Rajalakshmi, Akhilesh K. Arora, Y.V.G.S. Murti. Physica E 11 (2001).
[13] P.Y.Yu, T. S. Jeong, T.S.Kim. Journal of the Korean Physical Society 36 (2000).
[14] S.N.Andrew, M. Smith. Acc Chem Res. 43 (2010).
[15] K.A.Velizhanin. A.C. Francesco Meinardi, Roberto Simonutti, Monica Lorenzon, Luca Beverina, Ranjani Viswanatha, Victor I. Klimov & Sergio Brovelli. Nature Photonics 8 (2014).
[16] Tsung-Hsuan Yu, Wei-Yun Cheng, Kang-Ju Chao, Shih-Yuan Lu. International Journal of Hydrogen Energy 38 (2013).